Maintaining and escaping feedback control in hierarchically organised tissue: a case study of the intestinal epithelium

Matthias M. Fischer,[1,*] Hanspeter Herzel,[1,†] and Nils Blüthgen[1,‡]

[1] *Institute for Theoretical Biology, Charité and Humboldt Universität zu Berlin, 10115 Berlin, Germany*

(Dated: June 11, 2021)

The intestinal epithelium is one of the fastest renewing tissues in mammals with an average turnover time of only a few days. It shows a remarkable degree of stability towards external perturbations such as physical injuries or radiation damage. Tissue renewal is driven by intestinal stem cells, and differentiated cells can de-differentiate if the stem cell niche is lost after tissue damage. However, self-renewal and regeneration require a tightly regulated balance to uphold tissue homoeostasis, and failure can lead to tissue extinction or to unbounded growth and cancerous lesions. Here, we present a mathematical model of intestinal epithelium population dynamics that is based on the current mechanistic understanding of the underlying biological processes. We derive conditions for stability and thereby identify mechanisms that may lead to loss of homoeostasis. A key results is the existence of specific thresholds in feedbacks after which unbounded growth occurs, and a subsequent convergence of the system to a stable ratio of stem to non-stem cells. A biologically interesting property of the model is that the number of differentiated cells at the steady-state can become invariant to changes in their apoptosis rate. Moreover, we compare alternative mechanisms for homeostasis with respect to their recovery dynamics after perturbation from steady-state. Finally, we show that de-differentiation enables the system to recover more gracefully after certain external perturbations, which however makes the system more prone to loosing homoeostasis.

Keywords: Cancer, Colon, Dedifferentiation, Intestinal epithelium, Regeneration, Tissue homoeostasis

* matthias.fischer@charite.de

† h.herzel@biologie.hu-berlin.de

‡ **Corresponding author** – nils.bluethgen@charite.de

I. INTRODUCTION

A tissue is said to be hierarchically organised if it consists of different cell types constituting a characteristic hierarchical structure. Generally, two classes of cells can be distinguished: Adult stem cells have an unlimited capacity of indefinite self-renewal, but also differentiate and thus directly or indirectly give rise to differentiated cells which perform the designated function of the tissue [1]. Additionally in cases of tissue damage and regeneration the dedifferentiation of differentiated cells back into cycling stem cells has been observed, for instance in case of the intestinal epithelium [2, 3], the airway epithelium [4], and the kidney epithelium [5]. In order to uphold the homoeostasis of such a tissue in the face of external perturbations, a tight regulation of the stem cell compartment is required. In case of tissue damage, stem cells need to increase proliferation according to tissue requirements; however over-proliferation of the stem cell compartment must be avoided in order to prevent unlimited growth [6]. Such a tight control seems to be maintained through specific feedback loops exerted by differentiated cells onto the stem cell compartment regulating the size of the latter [7]. In contrast, control of the dedifferentiation of differentiated cells seems to be exerted by the stem cell compartment (see Tata *et al.* [4], and Beumer and Clevers [8] as well as the references therein). Escaping one or multiple of these stability-conferring control mechanisms may cause the tissue to loose homoeostasis and subsequently switch to a behaviour of unbounded, malignant growth.

The intestinal epithelium and the colon epithelium are prime examples of such hierarchically organised tissues. Despite its single-layered, simple epithelial structure it is able to withstand continuous mechanical, chemical and biological insults due to its specific tissue architecture in combination with a high rate of cellular turnover [9]: Stem cells residing at the bottom of the intestinal crypts cycle continuously approximately once per day and give rise to new cells. These cells then mature while migrating upwards, until they terminally differentiate and become part of the villi, eventually committing apoptosis and being shed off into the intestinal lumen [10]. Control of the intestinal and the colon stem cell compartment is realised via differentiated epithelial cells releasing Indian Hedgehog (Ihh), which stimulates mesenchymal cells to release Bone Morphogentic Proteins (BMPs). These, in turn, interfere with intracellular effects of WNT signalling and thus stimulate stem cell differentiation [11–15].

Previous theoretical research on hierarchically organised tissues has often focussed on the abstract case of arbitrary tissues: Rodriguez-Brenes *et al.* [16] considered arbitrary hierarchically organised tissues consisting of two compartments: a compartment of cycling and differentiating stem cells, and a compartment of non-cycling differentiated cells committing apoptosis at a fixed rate. They assumed that the differentiated cell compartment may exert feedback onto the stem cells by both decreasing their rate of proliferation and by reducing the probability of a stem cell division resulting in two daughter stem cells compared to the probability of a division yielding two differentiated cells. They then studied the order in which mutations in these feedbacks need to arise in a single new clone to enjoy a selective advantage and spread throughout the system. Limiting their model to sigmoidal *Hill*-like feedback functions, they then also fitted their model to a number of time-course data of the overall population size of growing tissue from the literature. The same model was used in Rodriguez-Brenes *et al.* [17] in order to reveal that during recovery from an injury significant damped oscillations in the path back to the steady-state may occur, and that this oscillatory behaviour is more pronounced when the stem cell load represents only a small fraction of the entire cell population. Nonetheless, oscillations may still be avoided, however at the price of slowing down the speed at which the system is able to recover after an injury. The same model topology has also been studied by Sun and Komarova [18] using the framework of a two-dimensional Markov process in order to obtain analytical solutions for the mean and variance of the cell compartment sizes. Recently, Wodarz [19] has extended the model by also taking into account the possibility of differentiated cells dedifferentiating into cycling stem cells again. Assuming sigmoidal *Hill*-like feedback onto stem cell cycling rate and self-renewal probability, he studied the effect of a linear and a sigmoidal dedifferentiation term, showing how unbounded, cancerous tissue growth may arise as a consequence of escaping this feedback. By means of numerical simulations, he also demonstrated how dedifferentiation may allow for speedier regeneration dynamics after perturbations.

More concrete theoretical studies have for example been carried out on the hematopoietic system [20–24], the mammalian olfactory epithelium [25, 26], or on the development, treatment and recurrence of breast cancer [27]. In contrast, however, theoretical examinations on the homoeostasis and dynamics of the intestinal and colon epithelium have been rare. A note-

worthy exception is Johnston *et al.* [28], who have derived and studied a three-compartment ODE model consisting of stem, transit-amplifying and terminally differentiated cells. They assumed that the first two of these three compartments limit themself either via a negative quadratic term (reminiscent of classical single-species population dynamic models which assume logistic growth [29]) or via a negative saturating term. However, no mechanistic justification of these models has been presented in the paper, possible also owing to the fact that our mechanistic understanding of the biology of intestinal stem cells has been rather limited until very recently [9].

In this work, we set out to derive a model of intestinal and colon epithelial population dynamics based on our current understanding of the involved underlying biological processes. We use this model in order to answer some fundamental questions about maintaining and losing the homoeostatic stability of this system: Both for the case without dedifferentiation and for the case with dedifferentiation, we derive all possible ways the system can loose stability and exhibit unbounded malignant growth. We prove analytically how allowing for dedifferentiation opens up an additional way of losing stability and switching to unbounded growth. For all cases of unbounded growth, we prove that – under the biologically reasonable assumption of saturating rate functions – after some period of transient behaviour the system will always converge to a stable ratio of cell types which we can calculate analytically. A special focus is given to the study of the transient behaviour of the system while recovering from different kinds of external perturbations. We examine how the shape of the feedback functions shapes the system behaviour during recovery, and will compare how graceful and efficient the colon model is able to recover from different kinds of external perturbations compared to other imaginable model topologies throughout the entire model parameter space. Finally, we show analytically and illustrate with numerical simulations how adding dedifferentiation can tremendously speed up recovery and reduce frequency and duration of oscillations, which especially applies to the case of perturbations of the stem cell compartment.

II. MATERIALS AND METHODS

A. Colon epithelium model

Our main model consists of two cell compartments S and D, denoting stem cells, and differentiated cells, respectively, following earlier approaches such as Rodriguez-Brenes *et al.* [16]. Stem cells cycle at a constant rate $\beta > 0$, whereas differentiated cells are cell-cycle arrested, but die with an apoptosis rate $\omega > 0$. Finally, stem cells differentiate with a rate $\delta(D)$ that is a function of the size of the differentiated cell compartment. Overall, the model is described by the following set of two coupled ordinary differential equations:

$$\begin{aligned} \frac{\mathrm{d}S(t)}{\mathrm{d}t} &= \beta S(t) - \delta(D)S(t) \\ \frac{\mathrm{d}D(t)}{\mathrm{d}t} &= \delta(D)S(t) - \omega D(t), \end{aligned} \tag{1}$$

where $\beta, \omega \in \mathbb{R}^+$ and δ is a continuously differentiable and monotonically increasing function $\mathbb{R}^+ \to \mathbb{R}^+$. A sketch of the model is shown in Figure 1a. Note that at this model does not include the possibility of dedifferentiation, and we will extend this later.

At this point, the structural similarity between our model and the classical Lotka-Volterra model of predator-prey dynamics [30, 31] may also be pointed out. In particular, if δ is a linear function with an intercept of zero, i.e. if the basal stem cell differentiation rate in the absence of differentiated cells is zero, then the models are mathematically identical. As remarked by Peschel and Mende [32], however, even such minor qualitative changes to the Lotka-Volterra model will affect its qualitative behaviour and cause the loss of its typical harmonic oscillations and for instance the emergence of a limit cycle or a stable steady-state instead.

B. Comparison of different model topologies

Next, we generalise the previous model to the family of all models containing exactly one explicit feedback loop from one compartment onto one rate parameter. Since we have two compartments which could potentially be able to exert a feedback (stem cells S, and differentiated cells D), and three rates which could potentially be affected by such a feedback

(stem cell proliferation, stem cell differentiation, and apoptosis of differentiated cells), we get a family of six possible models. It may be noted that this enumeration does not include any additional implicit feedback loops which may for instance arise as a consequence of enzyme sequestration [33]. We will compare these six models with each other with respect to their relaxation dynamics after perturbations.

C. Numerical simulations

Numerical simulations have been implemented in the Python programming language [34], version 3.7.3. All computations have been carried out on a 64-bit personal computer with an Intel Core i5-3350P quad-core processor running Manjaro Linux, kernel version 5.6.11-1.

We provide the complete commented source code of our numerical examinations in the form of an iPython juypter notebook in the following github repository: `https://github.com/Matthias-M-Fischer/Epithelium`.

D. Colon epithelium model with dedifferentiation

Finally, we extend the model by a dedifferentiation process of differentiated cells into stem cells. We model the rate of such a dedifferentiation to be determined by the size of the stem cell compartment, where a higher number of stem cells reduces dedifferentiation. Introducing an differentiable and monotonically decreasing function $\varrho : \mathbb{R}^+ \to \mathbb{R}^+$ describing the rate of dedifferentiation, the model reads:

$$\begin{aligned} \frac{\mathrm{d}S(t)}{\mathrm{d}t} &= \beta S(t) - \delta(D)S(t) + \varrho(S)D \\ \frac{\mathrm{d}D(t)}{\mathrm{d}t} &= \delta(D)S(t) - \varrho(S)D - \omega D(t). \end{aligned} \tag{2}$$

A sketch of the model is shown in Figure 4a.

III. RESULTS

A. A population dynamics model of the colon epithelium

We developed a model of the intestinal epithelial population dynamics (see Fig. 1a for a schematic overview, and Materials and Methods). The model distinguishes between two compartments: Stem cells that cycle at a rate β and differentiate at a rate $\delta(D)$, and differentiated cells that commit apoptosis and leave the system at a rate ω. We model the differentiation rate as a positive function of the size of the differentiated cell compartment D.This reflects the results of experimental studies demonstrating that differentiated cells release Indian Hedgehog (*Ihh*) that leads to an increased mesenchymal release of Bone Morphogenic Protein (*BMP*), which in turn stimulates the differentiation of intestinal stem cells [11, 12].

1. *Stability can be lost via two routes*

First we study the steady-states of system (1). For now, we will not use any specific function δ and only demand that δ is a positive, monotonic and continuously differentiable function. We also assume $\mathrm{d}\delta/\mathrm{d}D \geq 0$, since differentiated cells stimulate stem cell differentiation.

By solving $\mathrm{d}S(t)/\mathrm{d}t = \mathrm{d}D(t)/\mathrm{d}t = 0$ we find two steady-states: A trivial steady-state ($\bar{S} = 0$, $\bar{D} = 0$) that exists under all parameter values. Under some conditions, also a non-trivial steady-state exists at $\bar{S} = \omega\bar{D}/\beta$ and $\bar{D} = \delta^{-1}(\beta)$. Here, δ^{-1} denotes the inverse function of δ. This non-trivial steady-state exists if the function δ can reach the value of β. Thus, this second steady-state is only present if the maximal differentiation rate is higher than the proliferation rate. It is interesting to see that the steady-state does not depend on the apoptosis rate ω. This is a biologically interesting property which we will return to later.

To address the stability of the steady-states, we investigate the Jacobian [35] of the system:

$$\mathbf{J} = \begin{pmatrix} \beta - \delta(D) & -S\delta'(D) \\ \delta(D) & S\delta'(D) - \omega \end{pmatrix},$$

which at the trivial steady-state has the eigenvalues $\lambda_1 = \beta - \delta(0), \lambda_2 = -\omega < 0$. Hence, the trivial steady-state is only stable, if the proliferation rate β is smaller than the basal differentiation rate $\delta(0)$.

At any non-trivial steady-state, the Jacobian is given by

$$\mathbf{J}_{s-s} = \begin{pmatrix} 0 & -S\delta'(\bar{D}) \\ \beta & S\delta'(\bar{D}) - \omega \end{pmatrix}.$$

The steady-state is stable if $\det \mathbf{J}_{s-s} > 0$ and $\operatorname{tr} \mathbf{J}_{s-s} < 0$ (Routh–Hurwitz criterion, see Strogatz [36]) , which leads to $0 < \delta'(\bar{D}) < \delta(\bar{D})/\bar{D}$.

These results reveal two routes of how the intestinal epithelium can lose homoeostasis and show altered qualitative behaviour (Fig. 1b): First, the tissue might show unbounded growth, which could be interpreted as the emergence of a cancerous lesion (Fig. 1b, second column). This occurs once the proliferation rate β exceeds the maximum differentiation rate δ_{max} (either by increased proliferation or decreased maximal differentiation). In this case, only the (unstable) steady-state $(0, 0)$ remains, and any positive perturbation of S away from it will lead to unbounded growth

Second, the steady-state $\bar{D} = \delta^{-1}(\beta)$ can get unstable if $\delta'(\bar{D}) < \delta(\bar{D})/\bar{D}$. In other words, at the steady-state the slope of the feedback function might exceed $\delta(\bar{D})/\bar{D}$. When this happens, the behaviour of the system depends on the feedback function. This can be illustrated with the following two examples:

First, consider a linear function of the form $\delta(D) = \delta_0 + \delta_{slope} D$. For instability, we require that $\delta'(\bar{D}) > \beta/\bar{D}$, hence the system will only be stable for a strictly positive intercept δ_0. This is biologically plausible, since the intercept denotes the basal differentiation rate of stem cells in the absence of any external stimuli, which can be expected to exceed zero. If, however, the intercept is zero then the fix point will not be stable. This case is equivalent to the classical Lotka-Volterra model of predator-prey population dynamics, exhibiting undampened oscillations. As second example, consider a sigmoid function of the form $\delta(D) = \delta_0 + \delta_{max} D^p/(D_{min}^p + D^p)$. For instability, we require that $\delta'(\bar{D}) > \beta/\bar{D}$.

Hence, at $p > 4\beta/\delta_{max}$ the steady-state loses its stability, and the system will show sustained oscillations.

2. *Exponential growth and convergence to a stable cell type ratio after escaping control*

Next, we want to analyse the behaviour of system (1) when no non-trivial steady-state exists and the system shows unbounded growth. This case corresponds to a tissue that has escaped homoeostatic control and has degenerated into a cancerous lesion. In our model, this occurs when β exceeds the maximum of δ. This implies that the feedback funtion δ has a maximum value $\delta_{max} < \beta$. Such saturation of the differentiation rate could arise from saturated signalling or thermodynamical constraints.

Interestingly, during such unbounded growth the system will always converge to a stable ratio of stem cells and differentiated cells ($S(t)/D(t) = \text{const}$ for $t \to \infty$). The dynamics of the system is then governed by the following differential equations:

$$\begin{aligned}\frac{\mathrm{d}S(t)}{\mathrm{d}t} &= (\beta - \delta_{max})S(t)\\ \frac{\mathrm{d}D(t)}{\mathrm{d}t} &= \delta_{max}S(t) - \omega D(t).\end{aligned}$$

We are able to directly solve such a linear system analytically by first solving $S(t)$, yielding a simple exponential function, and subsequently solving $D(t)$. Overall, we get:

$$\begin{aligned}S(t) &= S_0 e^{(\beta-\delta_{max})t}\\ D(t) &= D_0 e^{-\omega t} + S_0\delta_{max}e^{-\omega t}\int_{s=0}^{s=t} e^{(\beta-\delta_{max}+\omega)s}\mathrm{d}s\,.\end{aligned}$$

Because the second term of $D(t)$ grows without bounds, we may for sufficiently big values of t neglect the decaying first term of $D(t)$. Calculating the integral then yields

$$D(t) = \frac{S_0\delta_{max}}{\beta - \delta_{max} + \omega}e^{(\beta-\delta_{max})t}\,.$$

This allows us to take the following limit

$$\lim_{t\to\infty}\frac{S(t)}{D(t)} = \frac{\beta+\omega}{\delta_{max}} - 1\,,$$

which denotes the ratio of stem to differentiated cells the system will converge to during explosive growth after some transient period.

Additionally, one may easily see that after the transient period, the overall growth of the system amounts to

$$S(t) + D(t) = S_0 \frac{\beta + \omega}{\beta + \omega - \delta_{max}} e^{(\beta - \delta_{max})t},$$

which implies an exponential growth at a constant rate $\beta - \delta_{max}$, which is also the dominant eigenvalue of the linear system. Figure 1c provides an exemplary numerical simulation of the system with a piecewise linear feedback function $\delta(D) = \min\{0.9 + 10^{-4}D, 1.0\}$, and parameters $\beta = 1.1$ and $\omega = 0.1$. Observe the convergence of the ratio $S(t)/D(t)$ to a stable ratio of $-1 + (\beta + \omega)/\delta_{max} \approx 0.2$, which is in agreement with our theoretical analysis.

3. Bifurcation analysis for the case of piecewise linear δ

Now, we want to further analyse the influence of system parameters on the qualitative and quantitative behaviour of system 1. To this end, we now chose a concrete differentiation rate function δ. For simplicity, we chose a piecewise linear function with a positive intercept $\delta_0 > 0$, denoting the basal differentiation rate of stem cells in the absence of any external cues. We assume that δ grows linearly in D with a slope of $\delta_{slope} > 0$, until it reaches an upper bound δ_{max}, at which point it stops increasing. Hence, we have

$$\delta(D) = \begin{cases} \delta_0 + \delta_{slope} D & \delta_0 + \delta_{slope} D \leq \delta_{max} \\ \delta_{max} & \text{else} \end{cases}, \tag{3}$$

where $\delta_0, \delta_{slope}, \delta_{max} > 0$.

The non-trivial steady-state resides at $\bar{S} = \omega \bar{D}/\beta, \bar{D} = (\beta - \delta_0)/\delta_{slope}$ and can only exist if $\beta < \delta_{max}$. The steady-state is only biologically feasible ($\bar{S}, \bar{D} > 0$) if $\delta_0 < \beta$. Then, the Jacobian at the steady-state is given by

$$\mathbf{J}_{eq} = \begin{pmatrix} 0 & -\frac{(\beta - \delta_0)\omega}{\beta} \\ \beta & \frac{(\beta - \delta_0)\omega}{\beta} - \omega \end{pmatrix},$$

which has the eigenvalues

$$\lambda_{1,2} = \frac{-\delta_0\omega \pm \sqrt{-4\beta^3\omega + 4\beta^2\delta_0\omega + \delta_0^2\omega^2}}{2\beta}.$$

If

$$\beta - \delta_0 < \frac{\delta_0^2\omega}{4\beta^2}$$

the radicand is positive. Then, due to $\delta_0 < \beta$ both eigenvalues will be negative and real, hence the steady-state is a stable node. If, however, the radicand is negative, oscillations occur and the real part of the eigenvalues is always negative due to $\delta_0 > 0$, making the steady-state a stable focus. In any case, any biologically feasible steady-state of this system will always be stable.

Biologically, it is interesting that no other constraints on δ_0 and δ_{slope} are required except for, $\delta_0 < \beta$, which we require for a feasible steady-state, and $\beta < \delta_{max}$. Particularly, $\delta_0 > 0, \delta_{slope} > 0$ can be arbitrarily small, yet the system remains stable. Similarly, changes in $\omega \geq 0$ will not affect the stability of the system. Figure 1d illustrates these findings and shows bifurcation plots of the system for varying parameters $\beta, \omega, \delta_0, \delta_{slope}$.

4. The feedback loop can cause oscillatory behaviour in cell numbers

Next, we investigated the behaviour when the system shows dampened oscillations around the steady-state. For any given steady-state $\bar{S}, \bar{D}$ it holds that $\delta_0 = \beta - \delta_{slope}\bar{D}$. This permits to express the eigenvalues $\lambda_{1,2}$, and thus the amplitude decay and the angular frequency of the dampened oscillations in terms of δ_{slope} instead of δ_0. We find that the amplitude of the oscillations will decay with

$$\sim e^{\frac{\delta_{slope}\bar{D}\omega - \beta\omega}{2\beta}t}.$$

Note that at any equilibrium the exponent is always negative because from $\bar{D} = (\beta - \delta_0)/\delta_{slope}$ it follows that $\delta_{slope}\bar{D} - \beta = -\delta_0 < 0$. The angular frequency of oscillations reads

$$\omega_0 = \sqrt{\delta_{slope}\bar{D}(4\beta^2\omega + \omega^2) - \beta\omega^2}/2\beta.$$

Hence, a higher slope of the feedback function δ will result in a slower decrease in the amplitude of oscillations, as well as cycle with a higher frequency. We provide a set of numerical simulations of the system with a piecewise linear function δ as defined before and varying values of δ_{slope} in Panel (e) of Figure 1 in order to illustrate our finding.

The relationship between function slope and oscillatory behaviour of the system is a biologically interesting result, as it suggests that in order to keep the occurring oscillations in check, a smaller slope of the feedback function might be desirable. For very small slopes, the difference between β and δ_0 needs to become sufficiently small as well, if the position of the steady-state $(\bar{S}, \bar{D})$ should remain constant. Then, the oscillations will complete vanish, and the steady-state becomes a stable node, as shown previously.

B. Comparison of different model topologies

In the previous section, we have shown that the colon epithelium model can cause homeostasis through a feedback from differentiated cells to stem cell differentiation. In the following, we explore how alternative feedback topologies in our two-compartment colon model might alter tissue homeostasis, and compare the properties of these models. We therefore generated all six one-looped topologies.

1. Controlling stem cells is required for stability

First, we consider those two topologies where the apoptosis rate ω is regulated by either the size of the stem cell compartment S or the size of the compartment of differentiated cells D, respectively. Both topologies are not able to show homoeostasis: If both the stem cell proliferation rate β and differentiation rate δ are unregulated and hence constant, we have $\mathrm{d}S(t)/\mathrm{d}t = \beta S - \delta S$, which for any non-trivial steady-state requires $\beta = \delta$. This, in turn, implies that $\mathrm{d}S(t)/\mathrm{d}t = 0$ at all points of time, hence after any perturbation of S, S will not

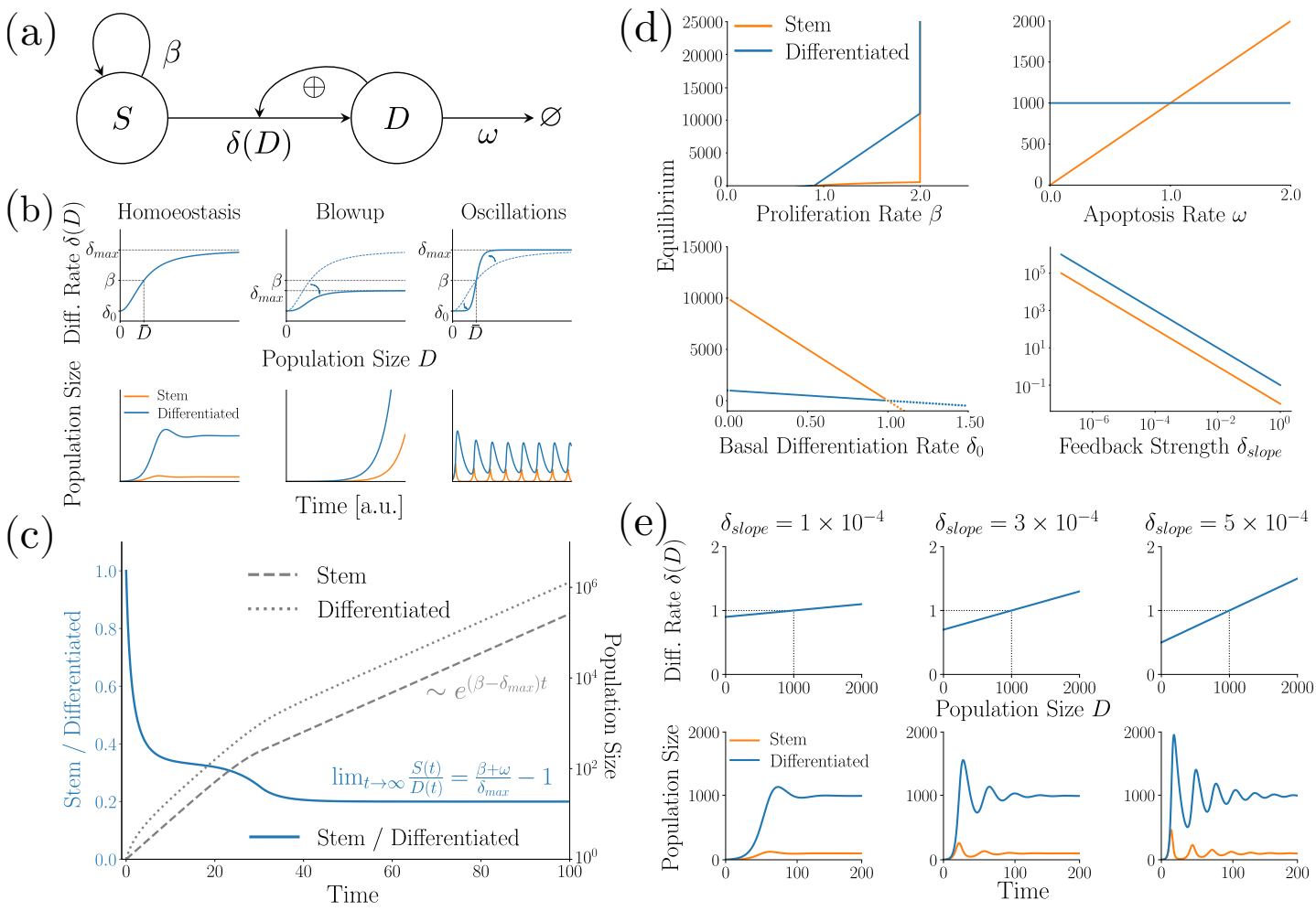

FIG. 1. The basic colon epithelium model. **(a)** Schematic sketch of the model. Stem cells S cycle at a rate β and differentiate at a rate $\delta(D)$ which is a positive function of the size of the differentiated cell compartment D. Differentiated cells commit apoptosis and leave the system at a rate ω. **(b)** The feedback function δ (upper row) determines the qualitative behaviour of the model (lower row). First column: Stable steady-state. Second column: the function δ has been altered to not map onto β any more, causing the destruction of the non-trivial steady-state and a switch to unbounded growth. Third column: at the steady-state, the function δ has a slope $\delta'(\bar{D}) > \beta/\bar{D}$, causing the steady-state to become unstable and the system to exhibit undampened, sustained oscillations. **(c)** In case of explosive growth, the system always converges to a stable ratio of stem to differentiated cells. Exemplary numerical integration. **(d)** Bifurcation diagram of the system with linear feedback function δ. Standard parametrisation: $\beta = 1.0, \omega = 0.1, \delta_0 = 0.9, \delta_{slope} = 10^{-4}, \delta_{max} = 2.0$. Note the switch from a stable steady-state to unbounded growth in the upper-left panel for $\beta > \delta_{max}$. Also note the invariance of the steady-state $\bar{D}$ to changes in apoptosis rate ω, shown in the upper-right panel. Both properties hold regardless of how we chose δ. Finally, notice that $\delta_0 > 0, \delta_{slope} > 0$ can be made arbitrarily small without ever losing stability and switching to unbounded growth; however, if δ_0 exceeds β, the non-trivial steady-state becomes unfeasible and unstable, and the system will always converge to the trivial extinction steady-state (lower two panels). **(e)** A steeper feedback functions causes stronger and longer oscillations. Shown here is a set of exemplary numerical simulations of the system with linear function δ for varying values of δ_{slope}, with the steady-state fixed at $\bar{S} = 100, \bar{D} = 1000$.

be able to return to its pre-perturbation state. Accordingly, these models are biologically

not realistic, and we will not consider them in the rest of this paper.

2. *Indirect regulation of the stem cell compartment decouples the steady-state number of differentiated cells from their apoptosis rate*

Next, we generalise our previous finding that in the colon epithelium model the steady-state $\bar{D}$ of differentiated cells is invariant to changes in ω to other model topologies. In fact, all models in which proliferation and differentiation of the stem cell compartment is exclusively regulated by the size of the differentiated cell compartment D following arbitrary continuously differentiable functions $\beta(D), \delta(D)$ enjoy this property: Let $\mathrm{d}S(t)/\mathrm{d}t = \beta(D)S - \delta(D)S$. At any non-trivial steady-state $(\bar{S}, \bar{D})$, from $\mathrm{d}S(t)/\mathrm{d}t = 0$ we get that $\beta(\bar{D}) = \delta(\bar{D})$. Define $\alpha(D) := \beta(D) - \delta(D)$, then $\bar{D} = \alpha^{-1}(0)$, which does indeed not depend on our choice of ω. This is biologically interesting since it is desirable from a physiological point of view to keep the number of differentiated cells as constant as possible, because differentiated cells are responsible for carrying out the primary function of a tissue. In contrast, $\bar{S} = \omega\bar{D}/\beta(\bar{D})$ depend linearly on ω. Also note that for the opposite case of a stem cell compartment which is only regulated by its own size, $\bar{S}$ is invariant to changes in ω, but $\bar{D}$ depends linearly on it.

3. *Saturating feedback functions β and δ cause convergence to a stable cell type ratio during unbounded growth*

Finally, it may also be briefly noted that all systems in which proliferation and differentiation rates of the stem cell compartment are functions saturating to β_{min} and δ_{max} for sufficiently big D respectively, will in case of unbounded growth converge to a stable ratio $S(t)/D(t) = \text{const}$ for $t \to \infty$, given as:

$$\lim_{t\to\infty} \frac{S(t)}{D(t)} = \frac{\beta_{min} + \omega}{\delta_{max}} - 1.$$

4. Differences in relaxation dynamics of different model topologies after perturbations

In this section, we compare the relaxation dynamics of the four remaining model topologies after applying external perturbations from steady-state, again using simple piecewise linear feedback functions to keep the analyses traceable. We will examine three different kinds of perturbations, which are: first, removing all differentiated cells; second, removing all but one stem cell; and third, both of these perturbations at the same time. Because of bilinear terms in the equations, we cannot in all cases obtain exact analytical solutions of the occurring dynamics, but use approximations of the dynamics based on a linearisation of the systems around their respective non-trivial steady-state (see Appendix A for details).

The Jacobian matrices and their eigensystems for the remaining four models are shown in Figure 2, along with schematic model sketches and exemplary numerical simulations, illustrating typical solutions.

Physiologically, it is important that the number of differentiated cells recovers quickly, as these are the cells responsible for carrying out the function of the respective tissue – for instance, the secretory and absorptive cells of the colon epithelium are all terminally differentiated cells. We hence compare the models based on their 'defect' χ of differentiated cells after perturbation – see Panel (a) of Figure 3 for an illustration. We define the defect as the total area between $D(t)$ after a perturbation at $t = 0$ and $\bar{D}$, i.e.

$$\chi := \int_{\substack{t=0 \\ D(t)<\bar{D}}}^{\infty} \bar{D} - D(t)\,\mathrm{d}t$$

.

The defect integrates only those time intervals in which $D(t) < \bar{D}$, as this defines the lack in functionality.

For all four models and the three types of perturbations, we derived either an analytical expression for the defect, or – if these are expressions too complicated for a meaningful analysis and interpretation – an approximate solution (see Appendix A). Three relations simplify their analysis: First, for all models we obtain $\omega = \beta\bar{S}/\bar{D}$. Second, the slope

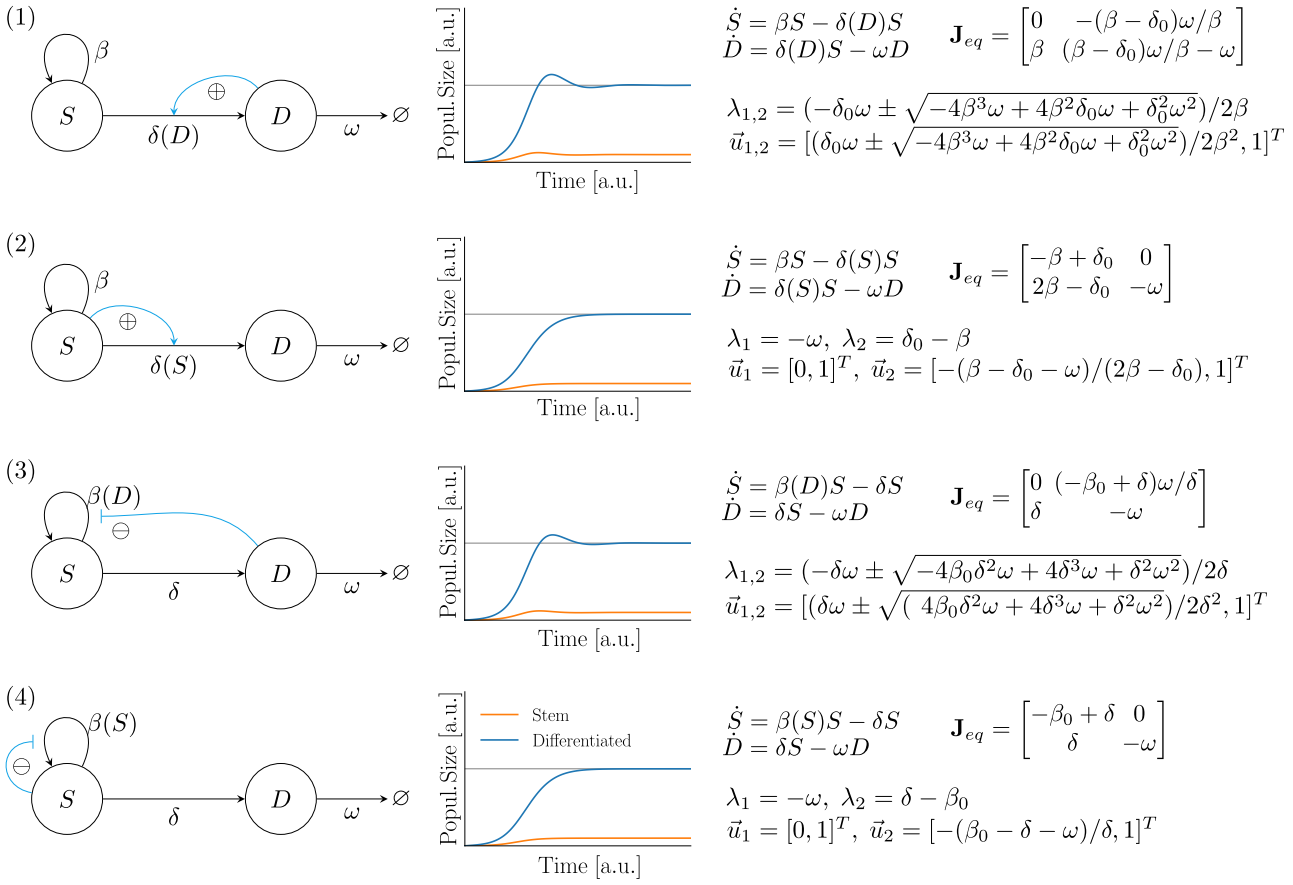

FIG. 2. All four one-looped model topologies that can show homoeostasis. First column: schematic sketches; second column: exemplary numerical simulations; third column: model equations, as well as Jacobian at the non-trivial steady-state and its eigensystem for the case of a linear feedback function $\beta(x) = \beta_0 + \beta_{slope}x$ or $\delta(x) = \delta_0 + \delta_{slope}x$, respectively.

of the feedback function (β_{slope} or δ_{slope}, respectively) is not required for describing the dynamics relative to the steady-state, as the slope is not part of the eigensystems of the steady-state Jacobians of the models. Third, we notice that the displacements of all models from steady-state of the first and second perturbation is linear in the initial displacement ($\Delta D(0)$ or $\Delta S(0)$, respectively). This indicates that in both cases the choice of initial displacement will not affect the comparison of the model defects, and we can express all defects as multiples of initial displacement. In case of the third perturbation, however, displacements are linear in $\Delta D(0)$, and contain an additional expression linear in $\Delta S(0)$. However, because at the steady-state the ratio of stem to differentiated cells is fixed, these two terms directly depend on each other, and we can express the defect as multiples of the

initial displacement of differentiated cells. Overall, this means the complete parameter space we need to consider consists only of the ratio of stem to differentiated cells at steady-state and two additional free parameters (depending on the model β_0, δ or β, δ_0).

a. Colon model vs. direct stimulation of stem cell differentiation We start by comparing our basic colon epithelium model, which is model 1 in our list, with model 2, where stem cell differentiation is not stimulated by the differentiated cell compartment, but instead by the stem cell compartment itself (see Panel (b) of Figure 3). Panel (c) of Figure 3 shows the difference in model defects throughout the parameter space (see Figures 5 and 6, Appendix B for the raw values), where areas shaded in red indicate region where our colon epithelium model has a bigger defect than the alternative model. In case of removing differentiated cells (first row) or removing both differentiated and stem cells at the same time (third row), there always exist ample regions (shaded in blue) where the colon model recovers more efficiently – namely, whenever the basal differentiation rate δ_0 of stem cells is close to the stem cell cycling rate β. This makes sense, because in case of the colon epithelium model removing differentiated cells will cause the stem cells to differentiate more slowly and thus grow in numbers quickly, thus being able to replenish the differentiated cell compartment more quickly. However, in case of removing only stem cells (second row), the colon epithelium model always performs worse than the alternative model, except for cases where the fraction of stem cells at the steady-state becomes sufficiently big (middle and right column). However, even then the difference between δ_0 and β still needs to be small for the colon model to recover more efficiently.

b. Colon model vs. indirect inhibition of stem cell cycling rate Next, we compare the recovery dynamics of the colon epithelium model with alternative model 3, where the differentiated cell compartment instead of stimulating stem cell differentiation inhibits stem cell cycling. Because the two models have different system parameters (β, δ_0 vs. β_0, δ) we cannot directly compare them pointwise in parameter space like we did before. However, we can still compare the ranges of model defects for the three different perturbations and steady-state stem cell fractions (1%, 10%, and 25%) if we systematically vary the two other free parameters of the models within biologically plausible intervals. In all cases, the defects of the colon epithelium model (Figure 5, Appendix B) and the defects of the alternative model (Figure 7, Appendix B) fall in similar ranges. Hence, there does not seem to be

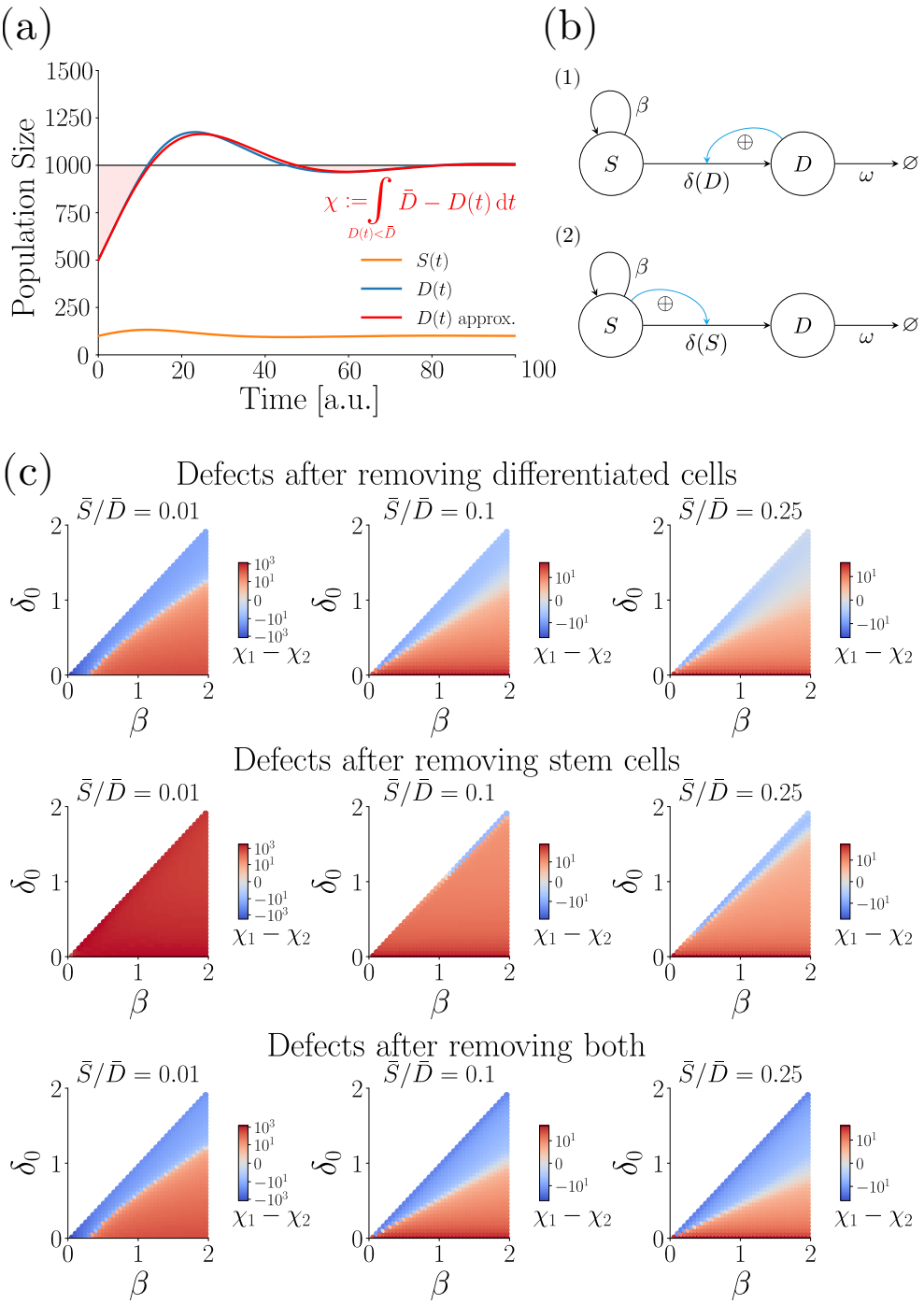

FIG. 3. **(a)** Illustration of our model comparison: After a perturbation at $t = 0$, the model relaxes to its steady-state (continuous blue and orange lines, depicting differentiated and stem cells, respectively). We use a first-order approximation (continuous red line) in order to not have to rely on costly numerical solutions of the system, and compute the 'defects' χ of the models we want to compare (shaded red area).**(b)**The two models we compare in this figure. Top: model 1, where stem cell differentiation is stimulated by the differentiated cell compartment; bottom: model 2, where the stem cell compartment stimulates its own differentiation. Note that model 1 is equivalent to our basic colon epithelium model derived earlier. **(c)** Difference in defects of model 2 and 1 throughout the parameter space. Areas shaded in red depict regions where model 1 shows a bigger defect, i.e. where the colon model recovers less gracefully than the alternative model; blue areas indicate the opposite. Columns represent different cases of stem cell fraction at steady-state (1, 10, and 25% respectively), rows represent the three different kinds of perturbations (removing differentiated cells, removing stem cells, and removing both, respectively).

any relevant difference between indirectly regulating stem cell differentiation vs. indirectly regulating stem cell cycling rate with respect to gracefully recovering from perturbations.

c. Colon model vs. self-inhibition of stem cell cycling rate Finally, we compare the recovery dynamics of the colon epithelium model with the behaviour of the remaining model 4, where the stem cell compartment inhibits its own cycling rate. In case of this comparison, we face the same problem of the two models having some different system parameters (β, δ_0 vs. β_0, δ) like in the previous section. We hence follow the same approach as before and compare the ranges of defects occurring in different scenarios. First, notice how in case of the first and third perturbation model 3 performs worse by up to several orders of magnitude if its stem cell differentiation rate δ is small (Figure 8, Appendix B). The only exception to this is the case of a very large steady-state stem cell fraction of 25%. This makes sense, since a small differentiation rate will cause the system to take a longer time to replenish the pool of differentiated cells, even more so if only a small amount of stem cells is present in the first place. In contrast, if differentiated cells are removed from the colon epithelium model, the stem cell differentiation rate will decrease, causing the stem cell compartment to temporarily grow quickly, until the growing differentiated stem cell compartment stimulates differentiation again. This way, the colon epithelium model is able to recover more quickly after removing differentiated tissue. For the remaining case of the second perturbation (removing stem cells), the model defects fall into similar ranges, however the colon epithelium model shows its largest defect in case of a small basal differentiation rate δ_0, whereas the alternative model performs the worst in case of a very small difference between basal stem cell proliferation rate β and differentiation rate δ. This does make sense, as in this case removing stem cells from model 1 will only cause a very small effective stem cell compartment growth rate of $\beta - \delta_0$, hence the model will take a long time to again completely replenish its stem cell compartment.

C. Dedifferentiation improves recovery from perturbations, however offers an additional route of losing homoeostasis

Previously, we have seen that in case of perturbations of the stem cell compartment, in a wide range of parameter values our colon epithelium model does not recover as gracefully as model

2, in which stem cell differentiation is stimulated directly by the stem cells themself (Figure 3, medium row). This is caused by the fact that in our colon epithelium model removing stem cells will not alter the rate of stem cell differentiation, since this rate is determined by the number of differentiated cells. Hence, removing stem cells will lead to a significant loss of differentiated cells first, before differentiation rate drops enough for the stem cell compartment to replenish itself, and subsequently replenish the compartment of differentiated cells. This way, the transient behaviour after removing stem cells is characterised by large oscillations in the number of differentiated cells, causing a large model defect.

We now study how allowing for the dedifferentiation of differentiated cells back into cycling stem cells affects these recovery dynamics of our colon epithelium model (see Panel (a) of Figure 4 for a schematic sketch of the updated colon epithelium model). We again assume for simplicity that the rate of stem cell differentiation is given by a linear function with intercept δ_0 and slope δ_{slope}. We also again assume that the function saturates to a maximum value δ_{max} after some value of D. Hence, we have $\delta(D) = \min\{\delta_0 + \delta_{slope} D, \delta_{max}\}$, where $\delta_0, \delta_{slope}, \delta_{max} > 0$. Next, we also for now assume the same, but horizontally mirrored shape for ϱ, giving $\varrho(S) = \max\{\varrho_0 + \varrho_{slope} S, \varrho_{min}\}$, where $\varrho_0 > 0, \varrho_{slope} < 0, \varrho_{min} \geq 0$.

For brevity purposes, we present the exact calculations in Appendix C. Briefly, adding a linear dedifferentiation function always causes a faster decay of the oscillations after perturbations. Additionally, we can find a critical value ϱ_0^*, which, when exceeded by ϱ_0 will reduce the frequency of oscillations after perturbations. It is given by

$$\varrho_0^* = (\beta - \delta_0/2)4\omega^2/\beta^2.$$

By means of a Taylor expansion around the steady-state, we can also generalise this finding to arbitrary decreasing differentiable functions ϱ.

Panel (b) of Figure 4 shows some exemplary numerical simulations of our colon epithelium model for the case of no dedifferentiation (first column), a linear dedifferentiation with $\varrho_0 = 0.5, \varrho_{slope} = -0.01$ (second column) and a faster linear dedifferentiation with $\varrho_0 = 0.9, \varrho_{slope} = -0.01$. (The other parameters are at their standard values of $\beta = 1$, $\omega = 0.1$, $\delta_0 = 0.9$, $\delta_{slope} = -10^{-4}$.) Observe, how the transient period after removing stem

cells is characterised by smaller oscillation amplitudes and frequencies dedifferentiation is allowed.

We also want to study the influence of dedifferentiation on the stability of the non-trivial steady-state of the system. Regardless of the concrete functions δ, ϱ, we find that the non-trivial steady-state needs to satisfy $\beta - \delta(\bar{D}) + (\beta/\omega)\varrho(\bar{S}) = 0$ and $\bar{D} = \beta\bar{S}/\omega$. Hence, a non-trivial steady-state exists, if and only if we can solve

$$\beta - \delta((\beta/\omega)\bar{S}) + (\beta/\omega)\varrho(\bar{S}) = 0, \bar{S} > 0, \tag{4}$$

which, importantly, shows that allowing for dedifferentiation enables the system to lose its non-trivial steady-state in another, new way, namely via a sufficient increase of the values of ϱ (see Panel (c) of Figure 4 for an illustration).

For the case of unbounded growth, it may also be pointed out that under the assumption of a saturating function ϱ converging to ϱ_{min} for sufficiently big values of S, the system will again converge to a stable cell type composition for $t \to \infty$, given by

$$\lim_{t\to\infty} \frac{S(t)}{D(t)} = \frac{a+b+w}{2d},$$

where $a := \sqrt{4dr + (b+w)^2}$ (see Appendix D for details).

IV. DISCUSSION

In this work, we have derived and analysed a population dynamics model of the colon epithelium, taking into account the stimulating effect of differentiated cells onto the differentiation of stem cells [11–15]. We revealed a number of general properties that hold regardless of the concrete feedback function: In case of any stable steady-state, the number of differentiated cells is not affected by changes in their rate of apoptosis, which is a biologically useful property, since differentiated cells are the cells responsible for carrying out the primary function of a tissue [1, 10] and changes in apoptosis rate may regularly happen locally as a consequence of infections or mechanical wounding [9]. Additionally, we have seen that strong alterations in system parameters are required for the homoeostatic steady-state to be destroyed and unbounded growth to occur – namely the stem cell proliferation rate needs to exceed all possible

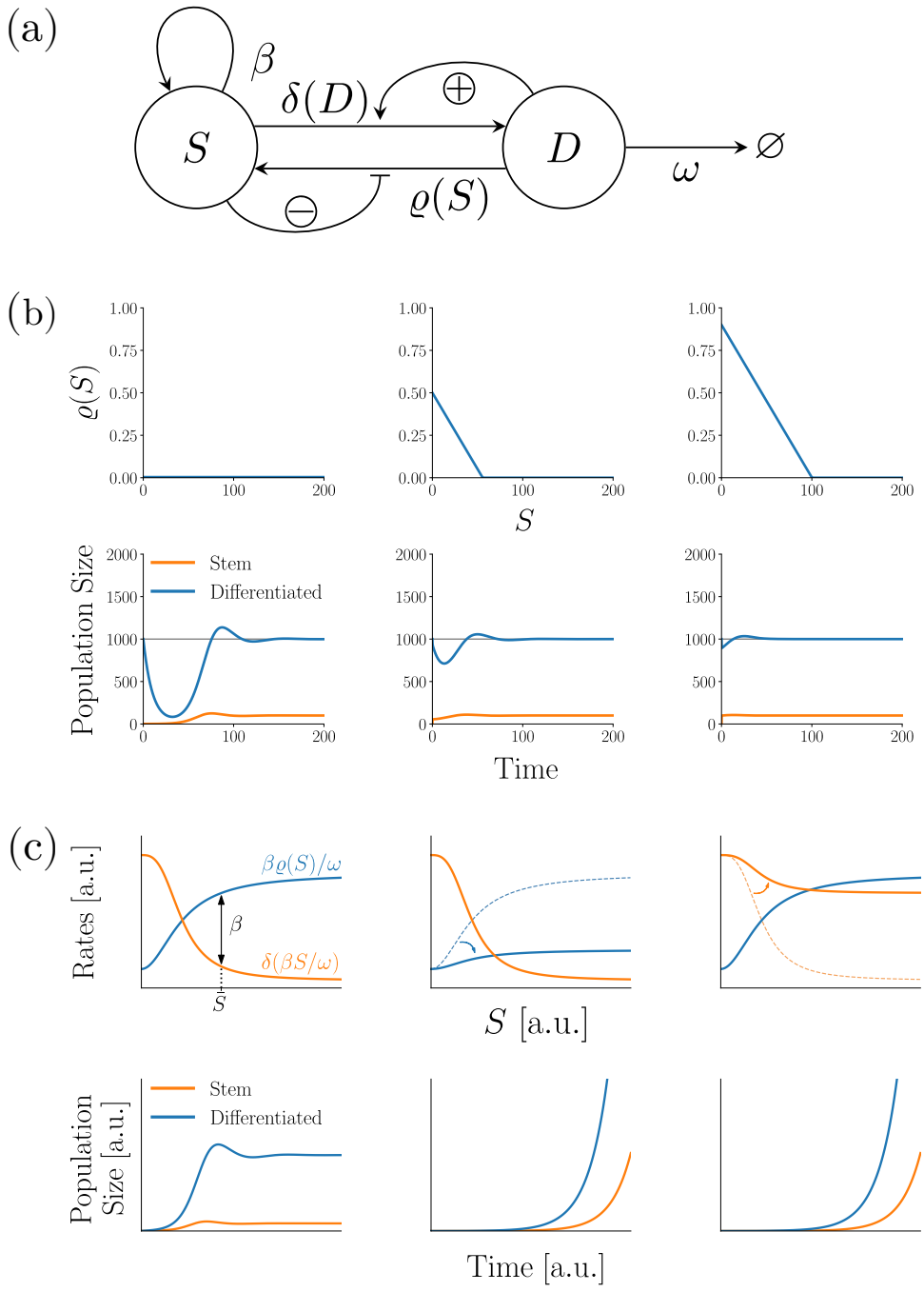

FIG. 4. The colon epithelium model with dedifferentiation and its most important properties. **(a)**: Schematic sketch of the model. **(b)**: Exemplary numerical simulations of the system with piecewise linear differentiation rate function δ and for different dedifferentiation rate functions ϱ. System parameters are $\beta = 1, \delta_0 = 0.9, \delta_{slope} = 10^{-4}, \omega = 0.1$. Note how adding dedifferentiation, as well as increasing the higher maximum dedifferentiation rate ϱ_0 makes the system recover more gracefully after removing stem cells. **(c)**: Adding dedifferentiation opens up a second way the system can lose homoeostatic stability. First column shows the case of homoeostasis. Equilibrium stem cell pool size $\bar{S}$ is given by solving $\beta\varrho(\bar{S})/\omega - \delta(\beta\bar{S}/\omega) = \beta$. Second column: Sufficient decrease of differentiation rate destroys the non-trivial steady-state and unbounded growth occurs. Third column: Sufficient increase of dedifferentiation rate has the same consequence.

values of the differentiation rate function. In contrast, any other single alteration, such as a moderate increase in cycling rate or a moderate suppression of dedifferentiation, is not able to cause unbounded growth, but will only change the position of the stable steady-state. This is equivalent to the case of a pre-cancerous lesion, where only a subset of 'canonical' colorectal cancer mutations is yet present and which shows a higher number of cells, but requires further genetic alterations to switch to unbounded growth [37]. Hence, our model recapitulates the observation of colorectal tumorigenesis being a characteristic multi-step process in vivo [38], showcasing the intrinsic resilience of the system towards mutations affecting system properties.

However, the advantages of an indirect feedback loop onto stem cell differentiation come with the drawback of possible oscillatory behaviour. Depending on the shape of the feedback function, more or – in case of a steeper function – less dampened oscillations around the steady-state may occur. This is reminiscent of e.g. the dampened oscillations observed in the healthy haematopoietic system [39]. In case of feedback functions with a high steepness around the steady-state, these oscillations can even become sustained and undampened. It is a well-known fact that systems with negative feedback loops may exhibit oscillations, even more so in the case of ultrasensitive feedback regulation (for example, see Kholodenko [40]). Hence the oscillatory behaviour of the colon epithelium model comes at no surprise from a mathematical point of view. However, such oscillations in cell numbers do not serve any immediately obvious biological purpose and indeed such oscillations may not be at all desirable for upholding tissue homoeostasis. This led us to the question whether this way of stabilising the system may offer additional beneficial properties compared to other ways of regulation.

We thus generalised the derived model to a family of all six imaginable one-looped model topologies. Two of them, namely those where the apoptosis rate of differentiated cells is controlled, cannot exhibit homoeostasis, showing that a mechanism controlling cycling stem cells is required for stability, be it in the form of controlling their proliferation rate, their differentiation rate, or potentially both. We have shown that if all of these control mechanisms originate exclusively from the differentiated cell compartment, the steady-state size of the differentiated cell compartment will still not be affected by changes in apoptosis rate. In contrast, if the stem cell compartment is exclusively regulated by itself, the steady-state density of stem cells, but not of differentiated cells will be unaffected by changes in apoptosis

rate. Because the differentiated cells are responsible for carrying out the designated function of a tissue [1], keeping their density as constant as possible is biologically desirable and thus grants systems with indirectly regulated stem cell compartments an advantage – even more so in tissues like the intestinal and colon epithelium which are constantly exposed to mechanical, chemical and biological insults [9].

We also revealed pronounced differences of the four stable model topologies regarding their ability to quickly return to their steady-state after external perturbations. We have shown the existence of ample regions in parameter space where the colon epithelium model recovers more gracefully from removing differentiated tissue compared to an alternative model, where stem cells stimulate their own differentiation. This makes sense because removing stem cells from the colon epithelium model cells will cause stem cells to differentiate more slowly. Hence the stem cell compartment can 'overshoot', until the growing compartment of differentiated cells forces more and more stem cells to differentiate. Thus, the differentiated cell compartment can be replenished quickly. However in case of removing stem cells, the colon model very often performed significantly worse since removing stem cells will not affect stem cell cycling and stem cell differentiation rates in the colon epithelium model. If, however, the differentiated cell compartment does not stimulate stem cell differentiation, but instead inhibits stem cell cycling, the recovery dynamics of the system do not seem to significantly change. Finally, if, in contrast, stem cells inhibit their own proliferation, the system generally performs worse compared to the colon epithelium model, regardless of which perturbation is applied. All in all, the colon epithelium model seems to generally show a significantly better or at least similar recovery behaviour compared to other model topologies except for the case of removing stem cells.

The inefficient relaxation dynamics of our colon model in case of stem cell removal prompted us to study the behaviour of our model if we additionally allow for dedifferentiation of differentiated cells back into cycling stem cells. We have shown both analytically and by exemplary numerical simulations how this enables the model to recover more gracefully from perturbations, especially those reducing the number of stem cells. Such a perturbations for instance represents the case of radiation-induced stem cell death [41]. However, adding the possibility of dedifferentiation to the system can also cause the destruction of the non-trivial

steady-state. This is biologically interesting, because it suggests that a sufficient increase in dedifferentiation rates may offer an alternative route of escaping homoeostatic control and entering a regime of unbounded, malignant growth of the tissue. Recent experimental data seems to indeed confirm this possibility of tumours arising from the differentiated intestinal epithelium as a consequence of inactivation of the differentiation-promoting transcription factor *SMAD4* [42]. Interestingly, mutations in *SMAD4* do indeed occur rather often in colorectal cancers [43, 44], suggesting that increased dedifferentiation might regularly contribute to colorectal tumorigenesis. Experimental data by Nakano *et al.* [45] points into the same direction, showing how dedifferentiation processes increase stemness in colorectal cancer.

Obviously, the introduction of the dedifferentiation term affects the steady-state position of the system, and one may easily verify (by writing Equation 4 in terms of $\bar{D}$) that its addition interferes with the invariance of the steady-state size of the differentiated cell compartment to changes in apoptosis rate. However, if the dedifferentiation rate around the steady-state is small and only becomes noticeable if a sizeable fraction of stem cells is removed (which seems to be suggested by the literature, see Tata *et al.* [4] and Beumer and Clevers [8]), then around the steady-state the dedifferentiation term becomes neglectable and the number of differentiated cells at steady-state stays invariant to changes in apoptosis rate.

We have also revealed that in case of a tissue which has switched to exhibiting unbounded growth, after a period of transient behaviour we will – under the biological reasonable assumption of saturating feedback functions – observe the convergence to a stable ratio of cycling stem cells and noncycling differentiated cells. This happens both in case of the colon epithelium model, as well as in case of all other studied model topologies, and is not affected by whether dedifferentiation of differentiated cells is possible or not. From a biological point of view, this is interesting because it directly relates to the topic of intratumoural heterogeneity [46–48], and suggest that after acquiring mutations and switching to unbounded growth the colon epithelium can still be expected to recapitulate known cellular hierarchies and differentiation gradients. In case of breast cancer [49] and cancers of the haematopoietic system [50] this has already been observed experimentally.

An interesting avenue for future research lies in the examination of healthy and tumoural

intestinal epithelial tissue on the single-cell level in order to answer the question, whether we are indeed able to identify similar cellular subpopulation and differentiation gradients in both of them. Very recent research seems to in fact suggest exactly this [51]. If this holds, tracking the numbers of different cell types over time during development and after perturbations would yield valuable data for validating and more accurately parametrising the model derived in this work. Additionally, comparing the quantitative behaviour of tissues in different stages of tumorigenesis could inform us at which of these stages which properties of the system are changed in which way compared to healthy tissue, and thus increase our mechanistic insight into the dynamics of tumour development. Such an increased mechanistic insight, in turn, might ultimately help to contribute to the development of novel approaches to limiting tumoural growth *in vivo*.

ACKNOWLEDGMENTS

We thank Christine Sers and Markus Morkel for fruitful discussions and helpful comments during an early stage of this project and DFG for funding (RTG2424, CompCancer).

AUTHOR DECLARATIONS

A. Conflicts of interest

All authors declare no conflict of interest.

B. Code availability

All source code for the reproduction of the numerical analyses is available in the following github repository: `https://github.com/Matthias-M-Fischer/Epithelium`

C. Author contributions

All authors conceived of the presented ideas; M.M.F. carried out model derivations and analyses with help from N.B. and input from H.H; M.M.F. produced the initial version of the manuscript with help from N.B; H.H. and N.B. contributed to the final version of the

manuscript; N.B. supervised the project. All authors have read and approve of the final version of this manuscript.

---

[1] I. L. Weissman, Stem cells: units of development, units of regeneration, and units in evolution, Cell **100**, 157 (2000).

[2] Y. Liu and Y.-G. Chen, Intestinal epithelial plasticity and regeneration via cell dedifferentiation, Cell Regeneration **9**, 1 (2020).

[3] Y. Liu, X. Xiong, and Y.-G. Chen, Dedifferentiation: the return road to repair the intestinal epithelium, Cell Regeneration **9**, 1 (2020).

[4] P. R. Tata, H. Mou, A. Pardo-Saganta, R. Zhao, M. Prabhu, B. M. Law, V. Vinarsky, J. L. Cho, S. Breton, A. Sahay, *et al.*, Dedifferentiation of committed epithelial cells into stem cells in vivo, Nature **503**, 218 (2013).

[5] J. V. Bonventre, Dedifferentiation and proliferation of surviving epithelial cells in acute renal failure, Journal of the American Society of Nephrology **14**, S55 (2003).

[6] B. Biteau, C. E. Hochmuth, and H. Jasper, Maintaining tissue homeostasis: dynamic control of somatic stem cell activity, Cell stem cell **9**, 402 (2011).

[7] F. M. Watt and B. L. Hogan, Out of eden: stem cells and their niches, Science **287**, 1427 (2000).

[8] J. Beumer and H. Clevers, Regulation and plasticity of intestinal stem cells during homeostasis and regeneration, Development **143**, 3639 (2016).

[9] H. Gehart and H. Clevers, Tales from the crypt: new insights into intestinal stem cells, Nature Reviews Gastroenterology & Hepatology **16**, 19 (2019).

[10] L. G. Van Der Flier and H. Clevers, Stem cells, self-renewal, and differentiation in the intestinal epithelium, Annual review of physiology **71**, 241 (2009).

[11] G. R. Van Den Brink, S. A. Bleuming, J. C. Hardwick, B. L. Schepman, G. J. Offerhaus, J. J. Keller, C. Nielsen, W. Gaffield, S. J. Van Deventer, D. J. Roberts, *et al.*, Indian hedgehog is an antagonist of wnt signaling in colonic epithelial cell differentiation, Nature genetics **36**, 277 (2004).

[12] B. B. Madison, K. Braunstein, E. Kuizon, K. Portman, X. T. Qiao, and D. L. Gumucio, Epithelial hedgehog signals pattern the intestinal crypt-villus axis, Development **132**, 279

(2005).

[13] L. E. Batts, D. B. Polk, R. N. Dubois, and H. Kulessa, Bmp signaling is required for intestinal growth and morphogenesis, Developmental dynamics: an official publication of the American Association of Anatomists **235**, 1563 (2006).

[14] W. A. Van Dop, J. Heijmans, N. V. Büller, S. A. Snoek, S. L. Rosekrans, E. A. Wassenberg, M. A. van den Bergh Weerman, B. Lanske, A. R. Clarke, D. J. Winton, *et al.*, Loss of indian hedgehog activates multiple aspects of a wound healing response in the mouse intestine, Gastroenterology **139**, 1665 (2010).

[15] N. V. Büller, S. L. Rosekrans, J. Westerlund, and G. R. van den Brink, Hedgehog signaling and maintenance of homeostasis in the intestinal epithelium, Physiology **27**, 148 (2012).

[16] I. A. Rodriguez-Brenes, N. L. Komarova, and D. Wodarz, Evolutionary dynamics of feedback escape and the development of stem-cell–driven cancers, Proceedings of the National Academy of Sciences **108**, 18983 (2011).

[17] I. A. Rodriguez-Brenes, D. Wodarz, and N. L. Komarova, Stem cell control, oscillations, and tissue regeneration in spatial and non-spatial models, Frontiers in oncology **3**, 82 (2013).

[18] Z. Sun and N. L. Komarova, Stochastic control of proliferation and differentiation in stem cell dynamics, Journal of Mathematical Biology **71**, 883 (2015).

[19] D. Wodarz, Effect of cellular de-differentiation on the dynamics and evolution of tissue and tumor cells in mathematical models with feedback regulation, Journal of theoretical biology **448**, 86 (2018).

[20] I. Roeder and M. Loeffler, A novel dynamic model of hematopoietic stem cell organization based on the concept of within-tissue plasticity, Experimental hematology **30**, 853 (2002).

[21] I. Glauche, M. Cross, M. Loeffler, and I. Roeder, Lineage specification of hematopoietic stem cells: mathematical modeling and biological implications, Stem cells **25**, 1791 (2007).

[22] I. Glauche, M. Horn, and I. Roeder, Leukaemia stem cells: hit or miss?, British journal of cancer **96**, 677 (2007).

[23] F. Michor *et al.*, Mathematical models of cancer stem cells, Journal of Clinical Oncology **26**, 2854 (2008).

[24] A. Marciniak-Czochra, T. Stiehl, A. D. Ho, W. Jäger, and W. Wagner, Modeling of asymmetric cell division in hematopoietic stem cells—regulation of self-renewal is essential for efficient repopulation, Stem cells and development **18**, 377 (2009).

[25] A. D. Lander, K. K. Gokoffski, F. Y. Wan, Q. Nie, and A. L. Calof, Cell lineages and the logic of proliferative control, PLoS Biol **7**, e1000015 (2009).

[26] W.-C. Lo, C.-S. Chou, K. K. Gokoffski, F. Y.-M. Wan, A. D. Lander, A. L. Calof, and Q. Nie, Feedback regulation in multistage cell lineages, Mathematical biosciences and engineering: MBE **6**, 59 (2009).

[27] H. Enderling, M. A. Chaplain, A. R. Anderson, and J. S. Vaidya, A mathematical model of breast cancer development, local treatment and recurrence, Journal of Theoretical Biology **246**, 245 (2007).

[28] M. D. Johnston, C. M. Edwards, W. F. Bodmer, P. K. Maini, and S. J. Chapman, Mathematical modeling of cell population dynamics in the colonic crypt and in colorectal cancer, Proceedings of the National Academy of Sciences **104**, 4008 (2007).

[29] P.-F. Verhulst, Notice sur la loi que la population suit dans son accroissement, Corresp. Math. Phys. **10**, 113 (1838).

[30] A. J. Lotka, Analytical note on certain rhythmic relations in organic systems, Proceedings of the National Academy of Sciences **6**, 410 (1920).

[31] V. Volterra, Fluctuations in the abundance of a species considered mathematically 1 (1926).

[32] M. Peschel and W. Mende, *The predator-prey model: do we live in a Volterra world?* (Springer, 1986).

[33] S. Legewie, B. Schoeberl, N. Blüthgen, and H. Herzel, Competing docking interactions can bring about bistability in the mapk cascade, Biophysical journal **93**, 2279 (2007).

[34] G. Van Rossum and F. L. Drake Jr, *Python tutorial* (Centrum voor Wiskunde en Informatica Amsterdam, The Netherlands, 1995).

[35] G. Jetschke, *Mathematik der Selbstorganisation* (Springer, 1989).

[36] S. H. Strogatz, *Nonlinear dynamics and chaos with student solutions manual: With applications to physics, biology, chemistry, and engineering* (CRC press, 2018).

[37] T. Muto, H. Bussey, and B. Morson, The evolution of cancer of the colon and rectum, Cancer **36**, 2251 (1975).

[38] E. R. Fearon and B. Vogelstein, A genetic model for colorectal tumorigenesis, cell **61**, 759 (1990).

[39] A. Marciniak-Czochra and T. Stiehl, Mathematical models of hematopoietic reconstitution after stem cell transplantation, in *Model Based Parameter Estimation* (Springer, 2013) pp.

191–206.

[40] B. N. Kholodenko, Negative feedback and ultrasensitivity can bring about oscillations in the mitogen-activated protein kinase cascades, European journal of biochemistry **267**, 1583 (2000).

[41] C. S. Potten and H. Grant, The relationship between ionizing radiation-induced apoptosis and stem cells in the small and large intestine, British journal of cancer **78**, 993 (1998).

[42] A. O. Perekatt, P. P. Shah, S. Cheung, N. Jariwala, A. Wu, V. Gandhi, N. Kumar, Q. Feng, N. Patel, L. Chen, *et al.*, Smad4 suppresses wnt-driven dedifferentiation and oncogenesis in the differentiated gut epithelium, Cancer research **78**, 4878 (2018).

[43] M. Miyaki, T. Iijima, M. Konishi, K. Sakai, A. Ishii, M. Yasuno, T. Hishima, M. Koike, N. Shitara, T. Iwama, *et al.*, Higher frequency of smad4 gene mutation in human colorectal cancer with distant metastasis, Oncogene **18**, 3098 (1999).

[44] N. I. Fleming, R. N. Jorissen, D. Mouradov, M. Christie, A. Sakthianandeswaren, M. Palmieri, F. Day, S. Li, C. Tsui, L. Lipton, *et al.*, Smad2, smad3 and smad4 mutations in colorectal cancer, Cancer research **73**, 725 (2013).

[45] M. Nakano, Y. Kikushige, K. Miyawaki, Y. Kunisaki, S. Mizuno, K. Takenaka, S. Tamura, Y. Okumura, M. Ito, H. Ariyama, *et al.*, Dedifferentiation process driven by tgf-beta signaling enhances stem cell properties in human colorectal cancer, Oncogene **38**, 780 (2019).

[46] M. Brattain, A. Levine, S. Chakrabarty, L. Yeoman, J. Willson, and B. Long, Heterogeneity of human colon carcinoma, Cancer and Metastasis Reviews **3**, 177 (1984).

[47] D. Buob, H. Fauvel, M.-P. Buisine, S. Truant, C. Mariette, N. Porchet, A. Wacrenier, M.-C. Copin, and E. Leteurtre, The complex intratumoral heterogeneity of colon cancer highlighted by laser microdissection, Digestive diseases and sciences **57**, 1271 (2012).

[48] C. K. Sievers, A. A. Leystra, L. Clipson, W. F. Dove, and R. B. Halberg, Understanding intratumoral heterogeneity: lessons from the analysis of at-risk tissue and premalignant lesions in the colon, Cancer prevention research **9**, 638 (2016).

[49] M. Al-Hajj, M. S. Wicha, A. Benito-Hernandez, S. J. Morrison, and M. F. Clarke, Prospective identification of tumorigenic breast cancer cells, Proceedings of the National Academy of Sciences **100**, 3983 (2003).

[50] D. Bonnet and J. E. Dick, Human acute myeloid leukemia is organized as a hierarchy that originates from a primitive hematopoietic cell, Nature medicine **3**, 730 (1997).

[51] W. R. Becker, S. A. Nevins, D. C. Chen, R. Chiu, A. Horning, R. Laquindanum, M. Mills, H. Chaib, U. Ladabaum, T. Longacre, *et al.*, Single-cell analyses reveal a continuum of cell state and composition changes in the malignant transformation of polyps to colorectal cancer, bioRxiv (2021).

Appendix A: Model dynamics after perturbations

Let $(\Delta S(0), \Delta D(0))$ denote a perturbation away from the steady-state $(\bar{S}, \bar{D})$ of a system at $t = 0$. Let $\vec{q}(t) = [\Delta S(t), \Delta D(t)]^T$ denote the dynamics of the displacement after the perturbation. We can approximate to first order $\mathrm{d}\vec{q}(t)/\mathrm{d}t \approx \mathbf{J}_{eq}\vec{q}(t)$, where $\mathbf{J}_{eq}$ denotes the Jacobian of the system at the steady-state. This linear system is then solved by $\vec{q}(t) = c_1 e^{\lambda_1 t}\vec{u}_1 + c_2 e^{\lambda_2 t}\vec{u}_2$, where $\lambda_{1,2}$ denote the eigenvalues of $\mathbf{J}_{eq}$, $\vec{u}_{1,2}$ denote their corresponding eigenvectors, and $c_{1,2} \in \mathbb{C}$ are to be chosen to satisfy the initial condition $\vec{q}(0) = [\bar{S} + \Delta S(0), \bar{D} + \Delta D(0)]^T$.

Because model 1 may show oscillations during its relaxation, an analytical calculation of its defects is theoretically possible, but leads to expressions too complicated to handle and meaningfully interpret. For this reason, we instead only derive the approximative relaxation dynamics of the model for the three perturbations and will calculate the corresponding model defects numerically. We get:

$$\Delta D_1(t) = \begin{cases} \Delta D(0)\dfrac{\cosh(rt) - (d/r)\sinh(rt)}{e^{dt}} & \text{First perturbation} \\ \Delta S(0)\beta\dfrac{\sinh(rt)}{re^{dt}} & \text{Second perturbation} \\ \Delta D(0)\dfrac{\cosh(rt) - (d/r)\sinh(rt)}{e^{dt}} + \Delta S(0)\beta\dfrac{\sinh(rt)}{re^{dt}} & \text{Third perturbation,} \end{cases}$$

where $d := \delta_0\omega/(2\beta)$, and $r := \sqrt{-4\beta^3\omega + 4\beta^2\delta_0\omega + \delta_0^2\omega^2}/(2\beta)$.

Next, we calculate the defects χ_2 of model 2 for the three perturbations. For the case of the first perturbation, the defect can be directly obtained by solving the system analytically for $S(0) = \bar{S}, D(0) = 0$ and calculating the integral. The other two defects are obtained by using the first-order approximation of the dynamics derived earlier and analytically calculating their integrals after choosing the respective initial conditions. We get:

$$\chi_2 = \begin{cases} \Delta D(0)\dfrac{1}{\omega} & \text{First perturbation} \\ \Delta S(0)\dfrac{2\beta - \delta_0}{\beta - \delta_0 - \omega}\left(1/(\delta_0 - \beta) + 1/\omega\right) & \text{Second perturbation} \\ \Delta D(0)\dfrac{1}{\omega} + \Delta S(0)\dfrac{2\beta - \delta_0}{\beta - \delta_0 - \omega}\left(1/(\delta_0 - \beta) + 1/\omega\right) & \text{Third perturbation.} \end{cases}$$

For model 3, we again only derive the relaxation dynamics after the three perturbations, and will examine them numerically. They are given by:

$$\Delta D_3(t) = \begin{cases} \Delta D(0)\dfrac{\cosh(rt) - (d/r)\sinh(rt)}{e^{dt}} & \text{First perturbation} \\ \Delta S(0)\dfrac{\delta \sinh(rt)}{re^{dt}} & \text{Second perturbation} \\ \Delta D(0)\dfrac{\cosh(rt) - (d/r)\sinh(rt)}{e^{dt}} + \Delta S(0)\dfrac{\delta \sinh(rt)}{re^{dt}} & \text{Third perturbation,} \end{cases}$$

where $d := \omega/2$, and $r := \sqrt{\omega(-4\beta_0 + 4\delta + \omega)}/2$.

For model 4, we can analytically calculate the defects after the three perturbations. They are:

$$\chi_4 = \begin{cases} \Delta D(0)\dfrac{1}{\omega} & \text{First perturbation} \\ \Delta S(0)\dfrac{\delta}{(\beta_0 - \delta)\omega} & \text{Second perturbation} \\ \Delta D(0)\dfrac{1}{\omega} + \Delta S(0)\dfrac{\delta}{(\beta_0 - \delta)\omega} & \text{Third perturbation.} \end{cases}$$

Appendix B: Model dynamics after perturbations

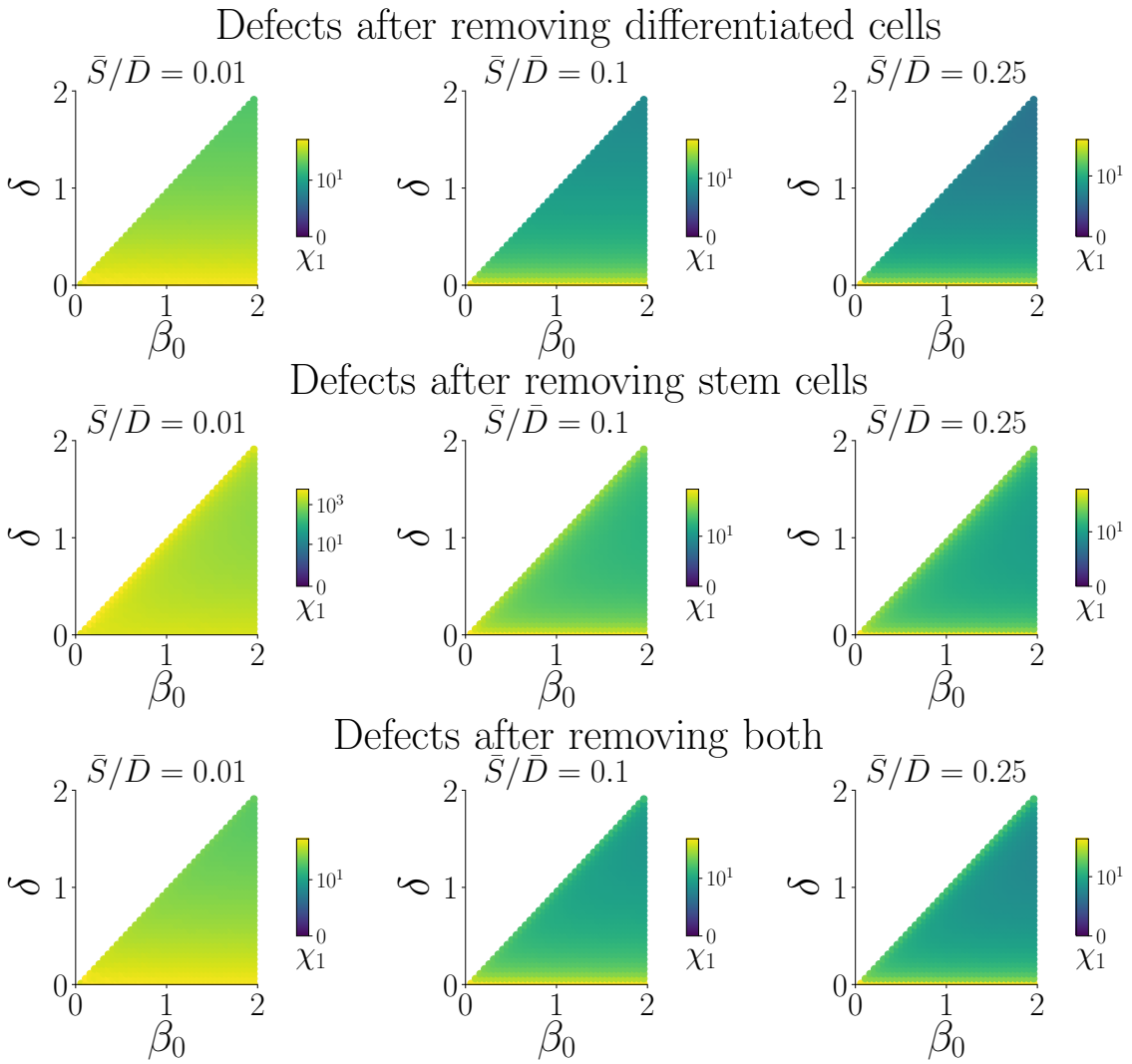

FIG. 5. The model defects χ_1 of model 1, the colon epithelium model, throughout its parameter space. Defects are given in multiples of initial perturbation size. Columns represent three different scenarios with different steady-state stem cell fractions of 1%, 10%, and 25%, respectively.

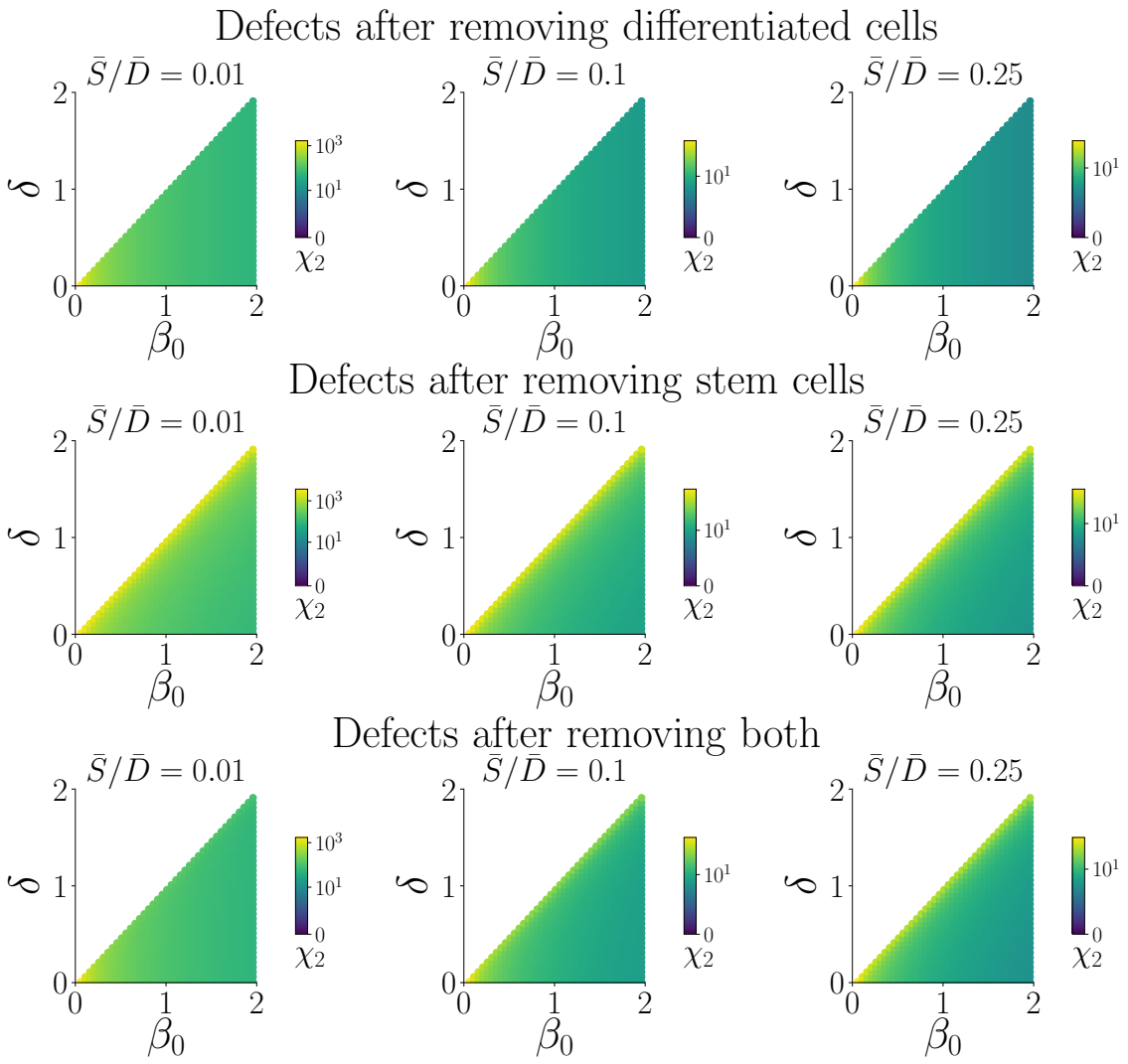

FIG. 6. The model defects χ_2 of model 1, the colon epithelium model, throughout its parameter space. Defects are given in multiples of initial perturbation size. Columns represent three different scenarios with different steady-state stem cell fractions of 1%, 10%, and 25%, respectively.

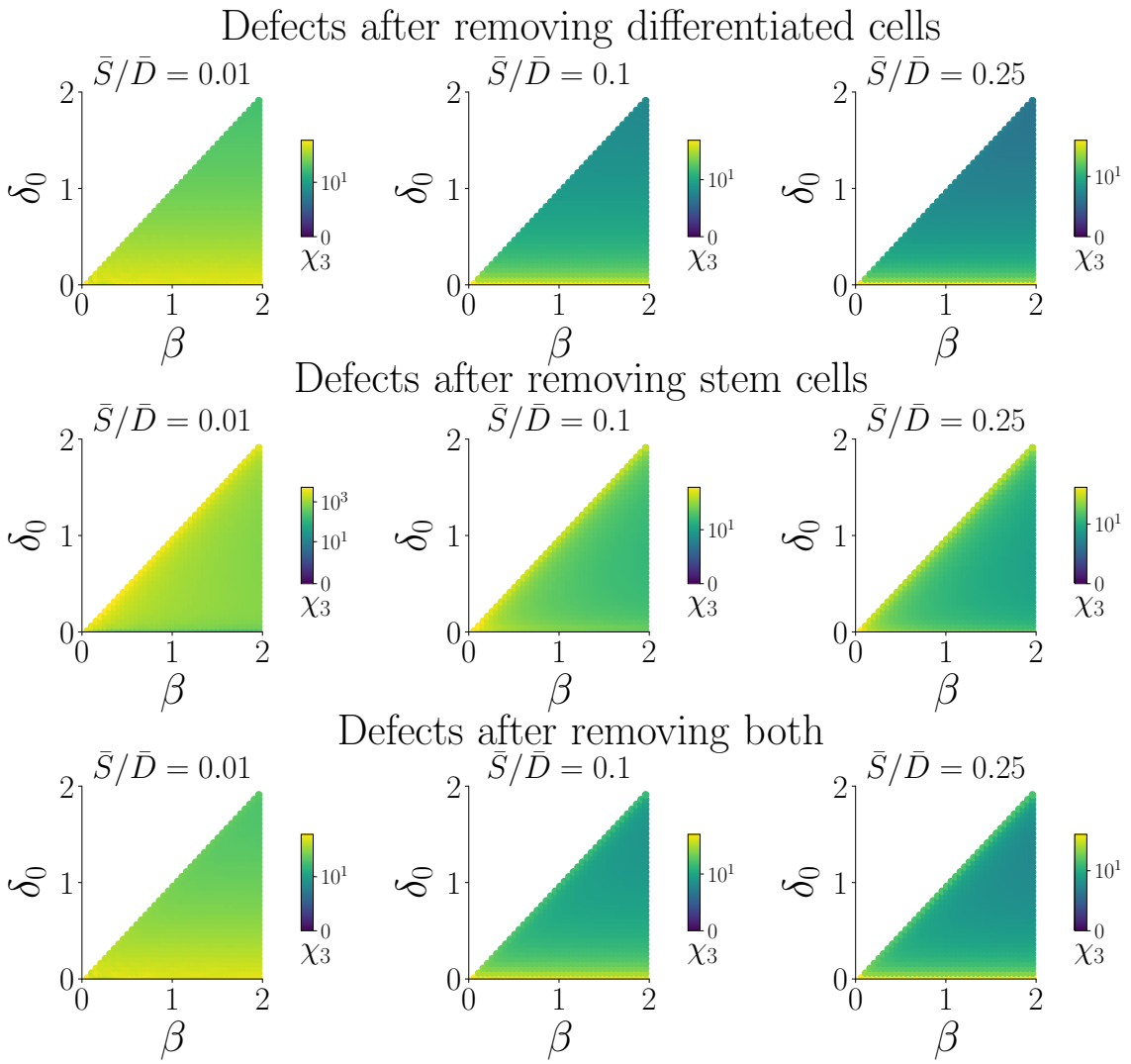

FIG. 7. The model defects χ_3 of model 3, where stem cell cycling rate is controlled by the number of differentiated cells, throughout its parameter space. Defects are given in multiples of initial perturbation size. Columns represent three different scenarios with different steady-state stem cell fractions of 1%, 10%, and 25%, respectively.

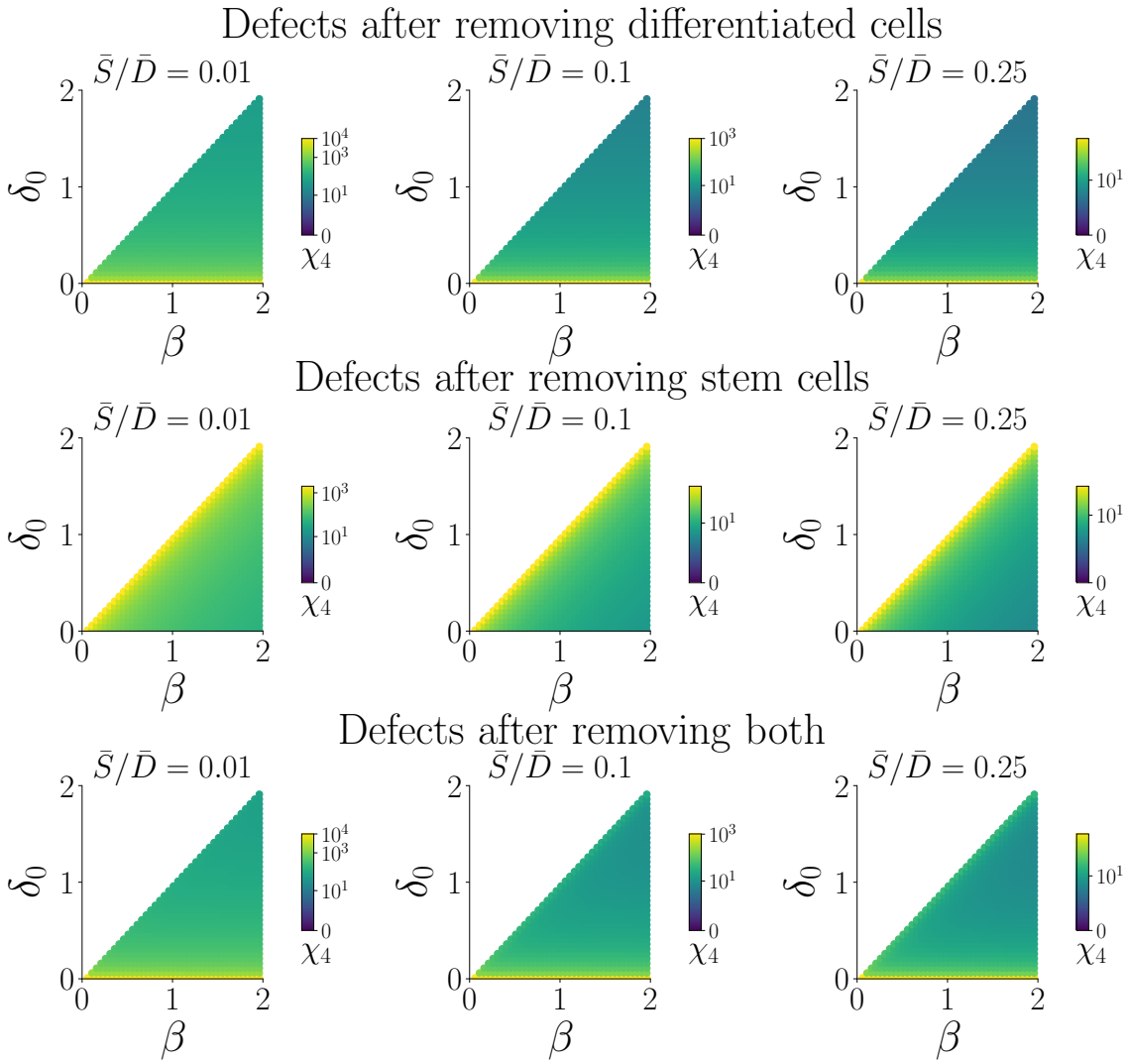

FIG. 8. The model defects χ_4 of model 4, where the stem cell compartment inhibits its own cycling rate, throughout its parameter space. Defects are given in multiples of initial perturbation size. Columns represent three different scenarios with different steady-state stem cell fractions of 1%, 10%, and 25%, respectively.

Appendix C: Dedifferentiation can limit oscillatory behaviour

The modified model permits exactly one non-trivial steady-state at

$$\bar{S} = -\frac{(\beta - \delta_0)\omega + \varrho_0\beta}{\beta(\varrho_{slope} - \delta_{slope})};\ \bar{D} = \beta\bar{S}/\omega,$$

and its Jacobian at this steady-state is given by

$$\mathbf{J}_{eq} = \begin{pmatrix} -\frac{\varrho_0\beta}{\omega} & -\frac{(\beta-\delta_0)\omega}{\beta} \\ \beta + -\frac{\varrho_0\beta}{\omega} & \frac{(\beta-\delta_0)\omega}{\beta} - \omega. \end{pmatrix}$$

This matrix has eigenvalues

$$\lambda_{1,2} = \frac{-\beta^2\varrho_0 - \delta_0\omega^2 \pm \sqrt{(\beta^2 - \varrho_0 + \delta_0\omega^2)^2 - 4(\beta^3\varrho_0\omega^2 + \beta^3\omega^3 - \beta^2\delta_0\omega^3)}}{2\beta\omega}$$

If oscillations occur, we have complex eigenvalues, which we can split into a real and an imaginary part as follows:

$$\Re(\lambda_{1,2}) = -\frac{\beta\varrho_0}{2\omega} - \frac{\delta_0\omega}{2\beta};\ \Im(\lambda_{1,2}) = \frac{\sqrt{(-\beta^2 - \varrho_0 + \delta_0\omega^2)^2 + 4(\beta^3\varrho_0\omega^2 + \beta^3\omega^3 - \beta^2\delta_0\omega^3)}}{2\beta\omega}.$$

For the colon epithelium model without differentiation the real part of the complex eigenvalues of the Jacobian at steady-state was given by $-\delta_0\omega/(2\beta)$. Accordingly, additionally allowing for dedifferentiation reduces the real part by $\beta\varrho_0/(2\omega) > 0$, hence always causing a faster decay of the oscillations after perturbations.

For the model without dedifferentiation we had an imaginary part of the eigenvalues of $\sqrt{4\beta^3\omega - 4\beta^2\delta_0\omega - \delta_0^2\omega^2}/(2\beta)$. Hence, adding the dedifferentiation to the model changes the radicand of the imaginary part of the eigenvalues by

$$\Delta = \beta\varrho_0 - \frac{\beta^2\varrho^2}{4\omega^2} - \frac{\varrho_0\delta_0}{2}.$$

Thus, we can find a critical value ϱ_0^*, which, when exceeded by ϱ_0 will reduce the frequency of oscillations after perturbations. It is given by

$$\varrho_0^* = (\beta - \delta_0/2)4\omega^2/\beta^2.$$

In other words, adding a linear dedifferentiation function will speed up the amplitude decay of the oscillations after perturbations and can also, in case of a sufficiently big basal dedifferentiation rate, decrease the frequency of these oscillations.

We can generalise this finding to arbitrary decreasing differentiable functions ϱ. To this end, we construct a Taylor expansion of ϱ around the steady-state of the form $\varrho(D) \approx a + bD + \mathcal{O}(D^2)$ with $a, b \in \mathbb{R}$. This way, in a sufficiently small neighbourhood around the steady-state, the system behaves as if ϱ was linear; and because ϱ by definition is always positive and monotonously decreasing, clearly $b < 0$ and accordingly $a > 0$. Hence, the argument for linear functions ϱ we made previously also applies here when we simply replace ϱ_0 with a.

Appendix D: Convergence of the colon epithelium model with dedifferentiation to a stable cell type ratio

For sufficiently high population sizes, the dynamics of the system are governed by the set of linear differential equations

$$\begin{aligned}\frac{\mathrm{d}S(t)}{\mathrm{d}t} &= \beta S(t) - \delta_{max} S(t) + \varrho_{min} D(t)\\ \frac{\mathrm{d}D(t)}{\mathrm{d}t} &= \delta_{max} S(t) - \varrho_{min} D(t) - \omega D(t).\end{aligned}$$

For convenience, we define $b := \beta - \delta_{max}, w := \omega + \varrho_{min}, r := \varrho_{min}, d := \delta_{max}$, giving

$$\begin{aligned}\frac{\mathrm{d}S(t)}{\mathrm{d}t} &= bS(t) + rD(t)\\ \frac{\mathrm{d}D(t)}{\mathrm{d}t} &= dS(t) - wD(t).\end{aligned}$$

This system has the general solution

$$S(t) = \frac{(a-b-w)S_0 - 2rD_0 + ((a+b+w)S_0 + 2rD_0)e^{at}}{2ae^{\frac{a-b+w}{2}t}}$$

$$D(t) = \frac{-2dS_0 + (a+b+w)D_0 + (2dS_0 + (a-b-w)D_0)e^{at}}{2ae^{\frac{a-b+w}{2}t}},$$

where $a := \sqrt{4dr + (b+w)^2}$. Taking the limit yields

$$\lim_{t\to\infty} \frac{S(t)}{D(t)} = \frac{a+b+w}{2d}.$$